

# Object-Based Morphometry of the Cerebral Cortex

J.-F. Mangin\*, D. Rivière, A. Cachia, E. Duchesnay, Y. Cointepas, D. Papadopoulos-Orfanos, D. L. Collins, A. C. Evans, and J. Régis

**Abstract**—Most of the approaches dedicated to automatic morphometry rely on a point-by-point strategy based on warping each brain toward a reference coordinate system. In this paper, we describe an alternative object-based strategy dedicated to the cortex. This strategy relies on an artificial neuroanatomist performing automatic recognition of the main cortical sulci and parcellation of the cortical surface into gyral patches. A set of shape descriptors, which can be compared across subjects, is then attached to the sulcus and gyrus related objects segmented by this process. The framework is used to perform a study of 142 brains of the International Consortium for Brain Mapping (ICBM) database. This study reveals some correlates of handedness on the size of the sulci located in motor areas, which was not detected previously using standard voxel based morphometry.

**Index Terms**—Atlas, brain mapping, cortical gyri, cortical sulci, pattern recognition.

## I. INTRODUCTION

ADVANCES in neuroimaging have led to an increasing recognition that certain neuroanatomical structures may be preferentially modified by particular cognitive skills or diseases. For cognitive studies, this point of view relies on the supposition that specialized or preferred behavior is associated with a commensurately greater allocation of neural circuitry in corresponding brain centers. For neurodegenerative disorders, the differential patterns of atrophy is supposed to reflect the clinical phenomenology [3]. This recognition has mainly resulted from the recent design of automated morphometric methods, which have empowered large-scale population studies [4], [74]. Therefore, brain morphometry is now one of the basic brain mapping tools at the same level as the various functional imaging modalities.

For most of the approaches, the automatic analysis relies on warping each brain toward a reference coordinate system, which plays the same role as the latitude and longitude system

for localization of points on the Earth's surface [27], [29], [30], [45], [71], [79]. The coordinate system is three-dimensional (3-D) for the comparison of the local densities of grey and white matter (voxel-based morphometry (VBM) [4]), or two-dimensional (2-D) (spherical) for the comparison of cortical thickness [26], [45]. Each new brain is endowed with one of these coordinate systems through *iconic spatial normalization*, namely a deformation matching as far as possible the new brain macroscopic anatomy as revealed by magnetic resonance imaging (MRI) with a template anatomy [21], [27], [30], [39]. The simplest approaches rely on affine transformations only, while modern registration techniques can now provide complex warpings relying on a large number of degrees of freedom, that are supposed to improve the normalization [13], [33], [37], [67]. Nonlinear warping can be the basis for deformation-based morphometry, a sibling of the tissue density morphometries which is also coordinate-oriented [17], [64], [65].

The iconic spatial normalization paradigm, originally introduced to overcome the poor statistics of positron emission tomography (PET) data [29], has made a tremendous impact on brain mapping strategies [55]. The coordinate-based approach, indeed, is very versatile since any dataset can be compared simply on a point-by-point basis. A disturbing fact, however, is that a number of different normalization algorithms are used throughout the world, each one potentially leading to different normalization results [22], [36]. Even SPM software proposes a lot of alternatives related to the size of the warping function basis or to the choice of the template [30]. This observation means that what is called spatial normalization is far to be clear simply because nobody really knows the gold standard of brain matching. Furthermore, nobody knows today to which extent matching two different brains with a continuous deformation makes sense from a neuroscience point of view.

The part of the brain leading to the main difficulties is the cortex, because the large variability of the folding patterns prevents the warping from attempting a perfect gyral matching across subjects [8], [36], [57]. Therefore, it seems rather difficult to perform reliable coordinate-based morphometric studies without either spatially blurring the data [4] or involving hundreds of subjects [32], [81]. A number of teams try to overcome current difficulties via more sophisticated iconic normalization procedures [73]. A significant improvement, for instance, consists in warping inflated cortical surfaces according to depth or curvature features, which simplifies the matching of the major sulci [27]. In our opinion, however, without a better understanding of the interindividual variability of the cortical folding patterns, the risk is the drift toward pure morphing techniques without consistent architectural justification. Spatial normalization, indeed, should try to match as far as possible the architectural parcellations of the cortical sheet [9]. Unfortunately, while some major sulci are usually considered

Manuscript received January 5, 2004; revised May 10, 2004. This paper is an extended version of a paper that appeared in the IPMI'03 proceedings [53]. The Guest Editors responsible for coordinating the review of this paper and recommending its publication were C. J. Taylor and J. A. Noble. *Asterisk indicates corresponding author.*

\*J.-F. Mangin is with the Service Hospitalier Frédéric Joliot, CEA, 91401 Orsay, France, the Institut Fédératif de Recherche 49, Paris, France, and INSERM ERM205, 91405 Orsay, France.

D. Rivière, E. Duchesnay, Y. Cointepas, and D. Papadopoulos-Orfanos are with the Service Hospitalier Frédéric Joliot, CEA, 91401 Orsay, France, and with the Institut Fédératif de Recherche 49, Paris, France.

A. Cachia is with the Service Hospitalier Frédéric Joliot, CEA, 91401 Orsay, France, the Institut Fédératif de Recherche 49, Paris, France, and with INSERM ERM205, 91405 Orsay, France.

D. L. Collins and A. C. Evans are with the Montreal Neurological Institute, McGill University, Montreal, QC H3A 2T8, Canada.

J. Régis is with the Service de Neurochirurgie Fonctionnelle et Stereotaxique, La Timone Hospital, 13006 Marseille, France.

Digital Object Identifier 10.1109/TMI.2004.831204

as good indicators of architectonic or functional transitions, few people postulate that this property can be extrapolated to all cortical folds [58], [82]. Anyway, the approaches imposing some sulcus-based constraints in the warping procedures [14], [16], [19], [35], [38], [72] seem more reasonable than blind morphing procedures only driven by image grey levels or surface curvature, even if some progress has to be made with regard to the automatic identification and the choice of the sulci to be matched.

In this paper, we advocate a complementary alternative to the coordinate-based point of view for the morphometry of the cortex. This alternative relies on a pattern recognition system performing first automatic detection of the sulci [62], and then parcellation of the cortical surface into gyri [12]. The definition of *various elementary objects* related to the cortical folding patterns allows the computation of a wide set of *local shape-based features* that can be compared across subjects [50]. Hence, this approach can be viewed as an automated version of a rather intuitive region of interest (ROI) based strategy. It should be noted that this ROI-based strategy is data-driven. Therefore, the ROIs actually fit individual anatomy. In contrast, the ROI-based strategy which warps a segmentation of the template brain [18], [20] suffers from the weakness of iconic normalization with regard to sulco/gyral patterns. This point will be addressed further in the discussion.

A first key point of the ROI-based strategy is that the combination of measurements gathering a subset of voxels increases the statistical power. This combination of measurements can simply rely on some averaging process, for instance through the computation of the mean thickness in a surface patch; but the ROI definition leads also to the emergence of new morphometric opportunities provided by various ROI-shape features. For instance the number and the types of interruptions of the major sulci, or the fact that two major sulci are connected or not, have never been correlated to cognitive features. The buried gyri leading to these interruptions [11], however, may be deeply correlated with the functional organization. This has been shown in the case of Broca's "pli de passage moyen," namely the gyrus buried in the central sulcus [7], [58], [87]. Some other interesting morphometric features are the depth and the surface of a given sulcus, which may give some clues about the development of the surrounding functional areas, because of the tensegrity principle: the idea that the folding reaches its final pattern via stabilization of the sum of tensions and compressions stemming from the different parts of the cortex (axone bundles, cortical mantle, etc...) [58], [78]. Hence, a second key point of the object-based strategy is the possibility to compare the various instances of the same anatomical entity without requiring a point-to-point warping, which may not exist. We do not claim that our approach provides miraculous solutions to the difficulties induced by the variability of the cortex folding patterns, but only a new window to compare the cortex shapes. The relevance of a sulcus-based parcellation system is supposed to stem from the complex links with the cortex architectony mentioned above.

This paper does not aim at providing a detailed description of the large battery of algorithms which is used to define sulci and gyri. Most of these algorithms, indeed, have been described previously elsewhere [12], [46]–[48], [51], [52], [62]. The goal of this paper is to provide an overview of the whole system, before focusing on the first meaningful neuroscience result obtained

within this framework. This paper is an extended version of the paper presented in IPMI'2003 [53]. The sulcus recognition module is the core of Section I and the gyrus-based geometric parcellation method is described in Section II. Then, Section III is dedicated to a simple study of the correlates of handedness relative to cortical asymmetries using a database of 142 brains of the ICBM project. This study reveals predictable correlates in the motor and premotor cortex which had not been found by a VBM study performed on the same database [81]. Finally, Section IV discusses the meaning of this result and some possible evolutions for cortex morphometry.

## II. AN ARTIFICIAL NEUROANATOMIST

The computer vision system in charge of the recognition of the cerebral sulci relies on a bottom-up strategy. This strategy aims mainly at using a scale of representation dedicated to the shape of the cortex. The transition toward a higher level stems from the conversion of each raw MR image into a structural representation supposed to embed all the information required for the sulcus recognition. While general purpose computer vision approaches build such representations from generic features like edges or corners, our approach relies on the cortical shape building blocks, namely the elementary folds [48]. Other similar methods have been proposed to break up the cortex into component parts related to the folds [15], [42], [44], [59], [63], [77], [88]. A rapid sketch of our conversion process is provided in Fig. 1. The underlying set of image processing tools and a dedicated visualization platform can be downloaded from <http://anatomist.info>. The framework has been applied successfully on more than 500 brains stemming from various scanners. The main steps of the *conversion process* are the following: (cf. Fig. 1).

- 1) The first step aims at restoring a meaningful link between intensity and class of tissue. Therefore, the spatial inhomogeneities induced by weaknesses of the acquisition process have to be overcome. This is achieved via the estimation of a smooth multiplicative field minimizing the entropy of the intensity distribution [46].
- 2) The next step is the analysis of the intensity distribution in order to infer the statistics of grey and white matter. A scale-space based approach provides robustness to the various variations observed across MR sequences and subjects [47].
- 3) Using the results of the previous analysis, the image is binarized in order to keep the range of intensities that may belong to the brain. A simple Markovian regularization adds robustness to this process. Mathematical Morphology is then used to define a mask of the brain. The binary image is eroded until a stage where the largest connected component does not intersect a layer of 5 mm defined from the outer surface of the head. This seed is then reconstructed using a conditional dilation in order to recover the brain shape [47].
- 4) A second sequence of erosion and conditional reconstruction is used to split the brain mask into hemispheres and cerebellum [52]. A white matter mask is defined first using a second regularized binarization. A virtual affine normalization to Talairach's space is then used to stop the erosion process which has to lead to the seeds.

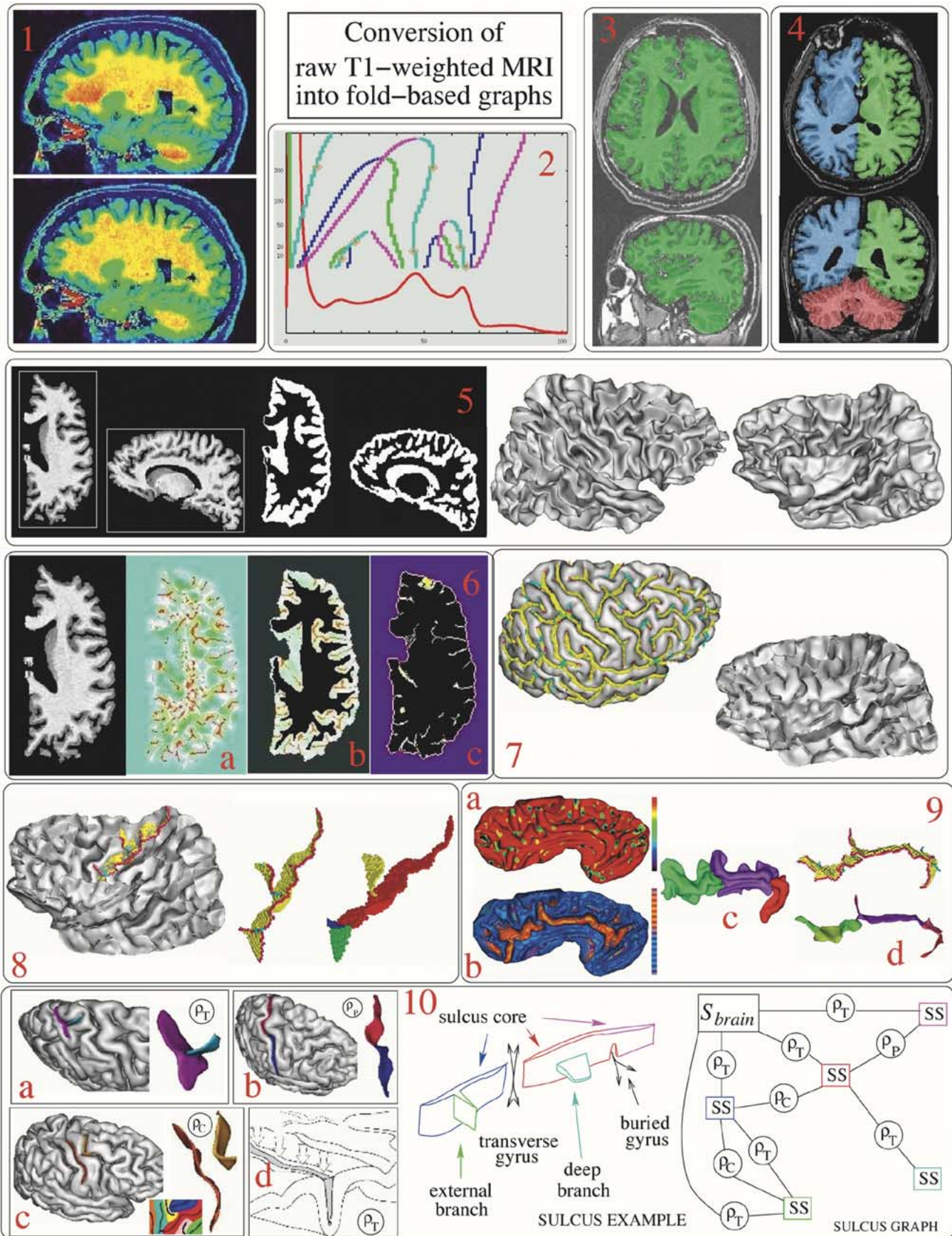


Fig. 1. Computation of a structural representation of the cortical folds from a raw T1-weighted MR image (cf. text).

A template image including another brain already split into the three targeted classes is used for this purpose. As soon as at least one large connected component is found included in each of the three template classes, erosion is stopped and a competitive reconstruction process begins. The seed selection process accepts seeds made up of several connected components, which turned out to be important to improve robustness.

- 5) The next step leads to the segmentation of the hollow object defined between the inner surface of the cortex and the brain hull. This hull is defined from a morphological closing, while the grey/white interface is defined relatively to the intensity statistics. A method based on topology preserving deformations imposes the spherical topology of this interface. This method which is based on a sequence of topologically simple points additions or deletions transforms the parallelepipedic bounding box of the hemisphere into the object of interest [48]. Fig. 1(5) provides 3-D rendering of the spherical grey/white interface from outside and from inside, namely from under the cortex.
- 6) Then, the hollow object is skeletonized. The erosion applied to compute the skeleton has not uniform speed. Indeed, to deal with variable cortex thicknesses on both sides of the fold, intensities are used to define the localization of the skeleton. Let us imagine that intensity is an altitude: white matter is crests and cerebro spinal fluid (CSF) is crevasses. To impose the skeleton localization in the depth of the crevasses, we use a “crevasse detector,” the mean curvature of the MR image isosurfaces [cf. Fig. 1(6.a)]. This detector amplifies the intensity differences, and overcomes situations where the fold does not include any CSF. This detector, however, is not perfect: some of the crevasse points are lost. The algorithm used to perform the skeletonization can fill the holes in the crevasse surfaces. This algorithm is a homotopic erosion which preserves the initial spherical topology of the hollow object. The behavior of this erosion looks like the effect of tide on sand castles. The extent of the castle at the beginning corresponds to the hollow object [cf. Fig. 1(6.b)] The castle altitude at each point corresponds to the crevasse detector answer. Each wave removes some sand of the castle outside walls. Little by little, the walls collapse under the water level. The highest parts of the castle are the last to collapse. When two water fronts meet, namely when a point becomes locally a surface point for discrete topology, a skeleton point is created [cf. Fig. 1(6.c)] [48].
- 7) Skeleton points connected to the outside are first gathered to represent the brain hull. The remaining part of the skeleton is classified into surface points (yellow), junction points (cyan) and edge point (red).
- 8) Surface points are gathered into topologically simple surfaces, namely pieces of surface which do not include any junction [48].
- 9) Each simple surface is split further in order to represent situations where a gyrus has been buried in the bottom of the fold. The underlying process computes first the Gaussian curvature of the MR volume isosurfaces. The Fig. 1(9.a) provides a glimpse of the Gaussian curvature

mapped on a part of the object inside interface. Then, each voxel of the hollow object connected to the inside and with a negative Gaussian curvature is deleted. A geodesic distance to the brain hull is computed inside the remaining part of the object [cf. Fig. 1(9.b)]. A system of catchment basins is finally computed from this geodesic depth [cf. Fig. 1(9.c)]. The buried gyri are supposed to create boundaries in this parcellation. Finally, each simple surface is split according to this parcellation [cf. Fig. 1(9.d)].

- 10) The resulting pieces of surface are gathered into a graph structure [48]. Fig. 1(10) gives an example where a sulcus is split into five pieces. Each node  $SS$  is a piece of the surface skeleton while  $S_{\text{brain}}$  represents the brain hull. Three kinds of relations are used: topological junction  $\rho_T$  [cf Fig. 1(10.a) and Fig. 1(10.d)], split induced by a buried gyrus  $\rho_B$  [cf Fig. 1(10.b)], neighbor geodesic to the brain hull  $\rho_C$ . This last kind of relation is inferred from a Voronoi diagram computed inside the brain hull using the junctions with the folds as seeds [Fig. 1(10.c)].

After the conversion process, the patterns of the cortex are represented by a *relational graph*, namely a set of elementary folds linked together according to their topographical organization relatively to junctions and proximity on the cortical surface. Various attributes are attached to the nodes and to the links of this graph in order to keep a sketch of the fold shapes. These attributes are computed after affine spatial normalization toward the standard proportional system [21]. This normalization can either be applied to the MR scan before the image processing step, or remain virtual, namely it is applied only to coordinates in the native scan. Some of these attributes are as follows [61]:

- fold*: size; maximal depth; center of mass; average normal; length, extremities and average direction of the intersection with the brain hull, etc.
- link*: direction between the centers of mass of the linked folds; length and average direction of the junction, etc.

At this stage the pattern recognition problem amounts to giving a name (or a label) from the sulcus nomenclature to each of these elementary folds. Our strategy for this purpose relies on supervised learning from a database of 26 manually labeled brains (see Fig. 2). Then, the system learns to generalize the knowledge embedded in this learning database across large variations of localization, orientation, and shape of the sulci. These variations are large enough to prevent reliable recognition using only localization in the proportional system [43]. But the main computational difficulty is the structural variability of the sulci across individuals. A sulcus corresponding to one very long elementary fold in one given brain may be made up of several small elementary folds in a second brain [11]. Furthermore, the junctions between sulci are also highly variable, which leads to difficulties similar to the ones related to the split of handwritten words into characters.

The structural variability of the sulci across brains can also be seen as analog to one of the difficult problems with which is confronted human vision: the variability of the spatial relationships among elementary parts of a complex object across orientation changes. An approach to tackle this difficulty consists in extracting a view-invariant structural description of the object

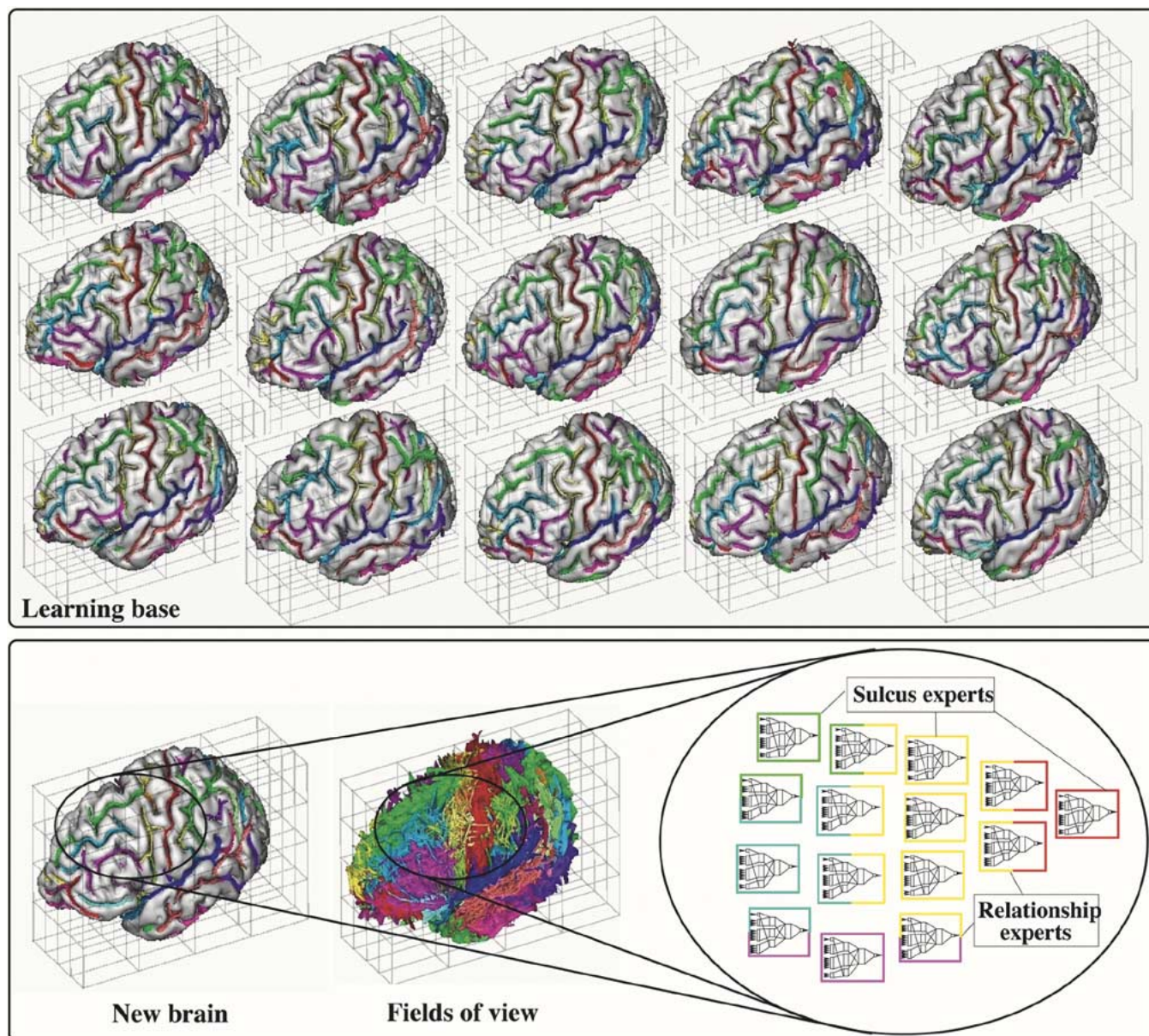


Fig. 2. The matching of the model of the cortical sulci with any new brain is performed according to a learning strategy. (top) The 15 brains of the learning database with manual labeling of some sulci. This database is used to train a congregation of 500 multilayer perceptrons [62]. Each brain of the database is aligned with the proportional system using an affine normalization. The proportional coordinate system, indeed, plays the role of the retinotopic coordinates in our artificial neuroanatomist. (bottom) Each perceptron is in charge of a local anatomical feature like the shape of a sulcus, or the shape of a pair of neighboring sulci. Each perceptron has a field of view which is the domain of the proportional system where the related feature appear in the database's brains. Automatic sulcus recognition is performed via stochastic minimization of the sum of the expert outputs, relatively weighted by their reliability on a test database.

that is then matched to stored object descriptions for recognition purpose [5]. Unfortunately, standard anatomical knowledge does not include any brain-invariant generic model of the sulci, which could be used to overcome the ambiguities when trying to label the elementary folds. Most of the psychological and physiological data, however, support a concurrent view-based human vision model, for which multiple views of each object are stored in memory [60]. We have designed our artificial neuroanatomist on the multiple-brain-based analog of this multiple-view-based approach: the shape of each sulcus is learned from a set of examples. Therefore, the resulting system is trained to mimic the interpretation of our human neuroanatomist, rather than to provide a putative gold standard of the sulcus recognition. Another neuroanatomist standing for a concurrent

interpretation of the folding patterns could provide a new manual labeling of the database that would lead to a rival artificial system.

The above discussion focuses on the notion of sulcus, which corresponds to a kind of character of the cortical fold alphabet inferred by the neuroanatomists of the last century. The emergence of these "characters" stemmed from the need to reduce the huge complexity of the cortex folding patterns to intermediate features, whose variability could be tackled by the human brain. This scale of representation may have been automatically selected to maximize the information delivered by the building blocks corresponding to a few examples of each sulcus [76]. Thank to this choice, the neuroanatomists get the capacity to generalize broadly to new brains.

A small number of sulci, in fact, have a shape stable enough to allow straightforward recognition. Usually, the other sulci are identified using a kind of vote collecting agreements about the presence of the surrounding sulci. This is a type of grouping process leading the neuroanatomist to recognize the patterns made up of a set of neighboring sulci. Furthermore, the neuroanatomist can only observe a subset of the sulci at the same time, which led us to design a Markovian system [31] relying only on local and contextual knowledge: the shapes of the individual sulci and the patterns made up by pairs of neighboring sulci. This choice relies on the assumption that a set of canonical local interactions between pairs of sulci is sufficient to model the patterns made up by more than two neighboring sulci. Each local anatomical knowledge is learned by a multilayer perceptron, which is a hyper-specialized anatomical expert. Two families of such experts are attached, respectively, to the sulcus shapes and to the neighborhood patterns (see Fig. 2). Memory-based longer range interactions may also be used by the neuroanatomist during the recognition. This may call for an extension of the set of interacting pairs in the future in order to take into account for instance the symmetric relationships across the interhemispheric plane.

Each sulcus expert of the first family has a field of view, which is learned from the database, and corresponds to a subvolume of the standard proportional system. This field of view is simply the bounding box of all the instances of the corresponding sulcus. During the labeling step corresponding to the recognition of the sulci of any new brain, the label corresponding to a given sulcus can only be given to the elementary folds included in the associated expert's field of view.

The set of pairs of sulci taken in charge by the second kind of perceptrons is also inferred automatically from the learning database. Each pair of sulci, whose instances in the database are sometimes linked, leads to the creation of a local expert dedicated to the resulting pattern. The contextual information driving the sulcus recognition stems from the sulcus neighborhood built by this second family of expert. The fields of view and this neighborhood endow the congregation of experts with a "corticotopic" organization, which may be related to the retinotopic or somatotopic organizations found in the cortex.

During the recognition step, each expert is in charge of giving an evaluation for a small part of the whole labeling. This evaluation ranges from zero (good) to one (bad). Sulcus experts deal with a subgraph of folds defined by one label, while pair experts deal with a subgraph of folds defined by two labels. The expert's evaluation is a measure of the likelihood of the shape made up by the folds of this subgraph, considering the *a priori* knowledge embedded into the learning database. In order to teach this knowledge to the perceptrons, each subgraph is compressed into a simple code made up of a fixed set of synthesized attributes. These attributes can be viewed as descriptors of the subgraph. Some are more syntactic, like the number of connected components; some others are semantic, like the total size or the maximal depth of the folds included in the subgraph. These synthesized semantic attributes are computed from the attributes attached to the elementary folds. Each perceptron is trained to give a good evaluation to the examples of the database, and a bad evaluation to random modifications of these examples. Each expert's reliability is assessed from a second learning base in order to weight the output of the expert before using it as a potential

of the global Markov field [62]. Finally, the automatic labeling of the folds of any new brain is driven by stochastic minimization of a global function made up of the weighted sum of the perceptron outputs.

The system is still at the beginning of its education. It has been trained from 16 manually labeled brains. Ten additional manually labeled were used: five brains as a test base preventing overlearning and five brains as a generalization base to perform a first evaluation. A nomenclature of 58 sulcus names is used in each hemisphere. The automatic recognition results decrease from 85% of accordance with the manual labeling on the learning base, to 75% on the generalization base, which calls for increasing the size of the learning base. It should be noted, however, that these results do not mean 25% of errors. Because of the large inter individual variability of the folding patterns, indeed, no gold standard exists to evaluate the percentage of correct labeling. This accordance measure, moreover, is highly dependent on the sulcus. For instance, the generalization leads only to 3.8% of disagreement for central sulcus; respectively, 6% for lateral fissure, while the disagreement may increase largely for more variable sulci, which leads sometimes to question the manual identification. It would be misleading, however, to over-interpret the respective rates of agreement obtained for each of the sulci [61] considering the small sizes of the databases. Therefore, it should only be kept in mind that the low quality of the identifications obtained for the most variable sulci is bound to hide some interesting features during the morphometric study described later.

The training of the 500 multilayer perceptrons on the base of 21 brains lasts about 12 h on a network of twenty recent Pentium processors. The stochastic minimization leading to the automatic labeling last one hour for one hemisphere with a 2 MHz processor and the default tuning of the temperature decreasing. While the results are close to the manual ones, a lot of questions remain open in the most variable cortical areas. Therefore, a future direction of work will consist in trying to improve the learning database manual labeling thank to a better understanding of the variability stemming from brain growth studies [11]. Another time consuming improvement could consist in performing several stochastic optimizations and keeping the labeling associated to the best result. Preliminary results have shown that this approach improves the rate of agreement [61]. Finally, increasing the size of the learning database is mandatory to increase the robustness of the recognition process.

### III. PARCELLATION OF THE CORTICAL SURFACE

Image analysis methods dedicated to the cortex almost always focus on cortical folds, because they can be defined simply using geometric properties. The usual neuroscience point of view about the cortical surface segregation, however, is gyrus based. A gyrus, indeed, is usually considered to be a *module of the cortex* endowed with dense axonal connections throughout local white matter (see [78]). Unfortunately, cortical gyri are relatively difficult to define from a pure geometrical point of view. Most of them, however, are assumed to be delimited by two parallel sulci. Therefore, our cortical surface parcellation is based on the previous sulcus recognition.

The main problem complicating the morphological definition of the gyri is the interruption of the delimiting sulci. The idea

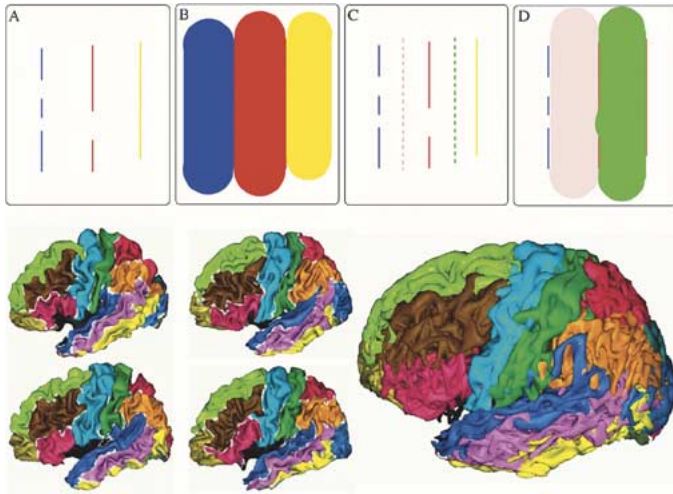


Fig. 3. (top) The definition of a gyrus from two parallel sulci using the Voronoi diagram principle. (A) Three schematic parallel sulci. (B) Definition of the Voronoi diagram of the sulcal lines, i.e. parcellation of the domain in influence zones of the sulci. (C) The boundaries between neighboring influence zones provides gyrus seeds. (D) A gyrus delimited by two parallel sulci can be obtained as the influence zone of the previous boundary seed. The initial sulcal lines are removed from the domain to prevent the front propagation underlying the Voronoi diagram construction to cross them (a gyrus should end at the bottom of the limiting sulci). The rest of the gyrus boundaries will be induced by a competition with the other gyri. (bottom) A typical parcellation obtained for the left hemisphere of four different brains. Each color corresponds to a different gyrus. The boundaries between gyri appear in white. For the external face of the brain, the set of pairs of sulci selected for this experiment aims at defining the three horizontal frontal gyri and the polar frontal face, the three horizontal temporal gyri, The precentral and postcentral vertical gyri corresponding to motor (cyan) and somesthetic (green) areas, and the two parietal lobules. Some non satisfying attempts have been done to parcellate the occipital lobe. The right image provides the mixing of six brains in the standard proportional system.

developed in our framework overcomes this difficulty using the Voronoi diagram principle (see [11]). Such a diagram is a parcellation of space from a set of seeds. Each parcel is the influence zone of one of the seeds, namely the domain of space closer to this seed than to any other seed. If a set of lines approximately located at the level of the crowns of the gyri of interest can be provided as gyrus seeds, the whole gyral parcellation can be defined from a geodesic distance computed geodesically to the cortical surface. Such seed lines can be extracted from the boundaries of a first Voronoi diagram computed using the projections of the sulcus bottoms on the cortical surface as seeds (see Fig. 3). In order to impose the sulcus bottoms as parts of the boundaries between the gyral influence zones, they are removed from the cortical surface during the computation of the second diagram to prevent the distances to be propagated across these lines. Hence the resulting diagram is inferred from an iterative dilation of the gyrus seeds that is stopped either at the level of the sulcus bottoms, or when two zones of influence get in touch with each other.

A few results of parcellation are presented in Fig. 3. These results are qualitatively comparable to atlas descriptions, apart in occipital lobe. The parcellation method assumes that a reliable identification of the main sulci can be performed first for any subject, which is far to be the case with the current pattern recognition system. We think, however, that the current state of this system is sufficient to obtain interesting morphometry re-

sults if a large database of brains is processed, which can now be done without any user interaction.

#### IV. CORRELATES OF HANDEDNESS

It is usually assumed that the loss of statistical power induced by the non perfect gyral matching of spatial normalization can be compensated by large population sizes. Two recent large-scale VBM studies with hundreds of subjects, however, have reported a surprising absence of results relative to the possible relationship between brain asymmetry and handedness [32], [81], which may reveal some limits of the point-by-point paradigm. Since human handedness can be viewed as a model of proficient or preferred behaviors, several ROI-based morphometric studies have also addressed this issue for a few cortical structures. For instance, the central sulcus, which houses the primary motor cortex, was found to be deeper in the left hemisphere in right-handers, and *vice versa* in left-handers [1], [2], [84]. This result remains controversial as other studies did not confirm this interaction [83] or found an inverse pattern [23]. Methodological differences and age effects may explain these inconsistencies [75].

To investigate whether the new observation window provided by our framework could answer the kind of issues addressed by these manual ROI-based studies, 142 unselected normal volunteers of the ICBM database were processed without any manual interaction. These subjects correspond to one of the VBM studies mentioned above [81]. On a short handedness questionnaire, 14 subjects were dominant for left-hand use on a number of tasks; the remaining 128 subjects preferred to use their right hand. The 142 T1-weighted brain volumes were stereotaxically transformed using nine parameters [4] to match the Montreal Neurological Institute 305 average template. A set of 58 cortical sulci were recognized in each hemisphere. In order to reduce the risk of large failure of the stochastic minimization leading to the sulcus recognition, the optimization was performed two times for each brain and the lowest minimum was selected for the morphometric study.

Among the various morphometric features used by the artificial neural networks to perform the recognition, four were chosen to compute simple asymmetry indexes (cf Fig. 4)

- *The number of voxels of the skeleton representing the sulcus.* This number can be compared across subjects because the MR images are normalized to a 1-mm resolution at the beginning of the conversion process. This measurement, however, is not straightforwardly related to the size of the sulcus because the sulcus orientation biases the discrete sampling.
- *The surface of the sulcus.* This measurement is supposed to overcome the weaknesses of the first one relative to the sulcus orientation. A marching cube type of algorithm is used to mesh the skeleton voxels. Then, the sum of the areas of the triangles of the resulting mesh is used to evaluate the sulcus surface. It should be noted that this measurement can not account for an opening of the sulcus induced for instance by atrophy.
- *The number of voxels of the junction between the sulcus and the brain hull.* This number is related to the length of the 3-D curve corresponding to the trace of the sulcus at the external surface of the brain. This measurement is also

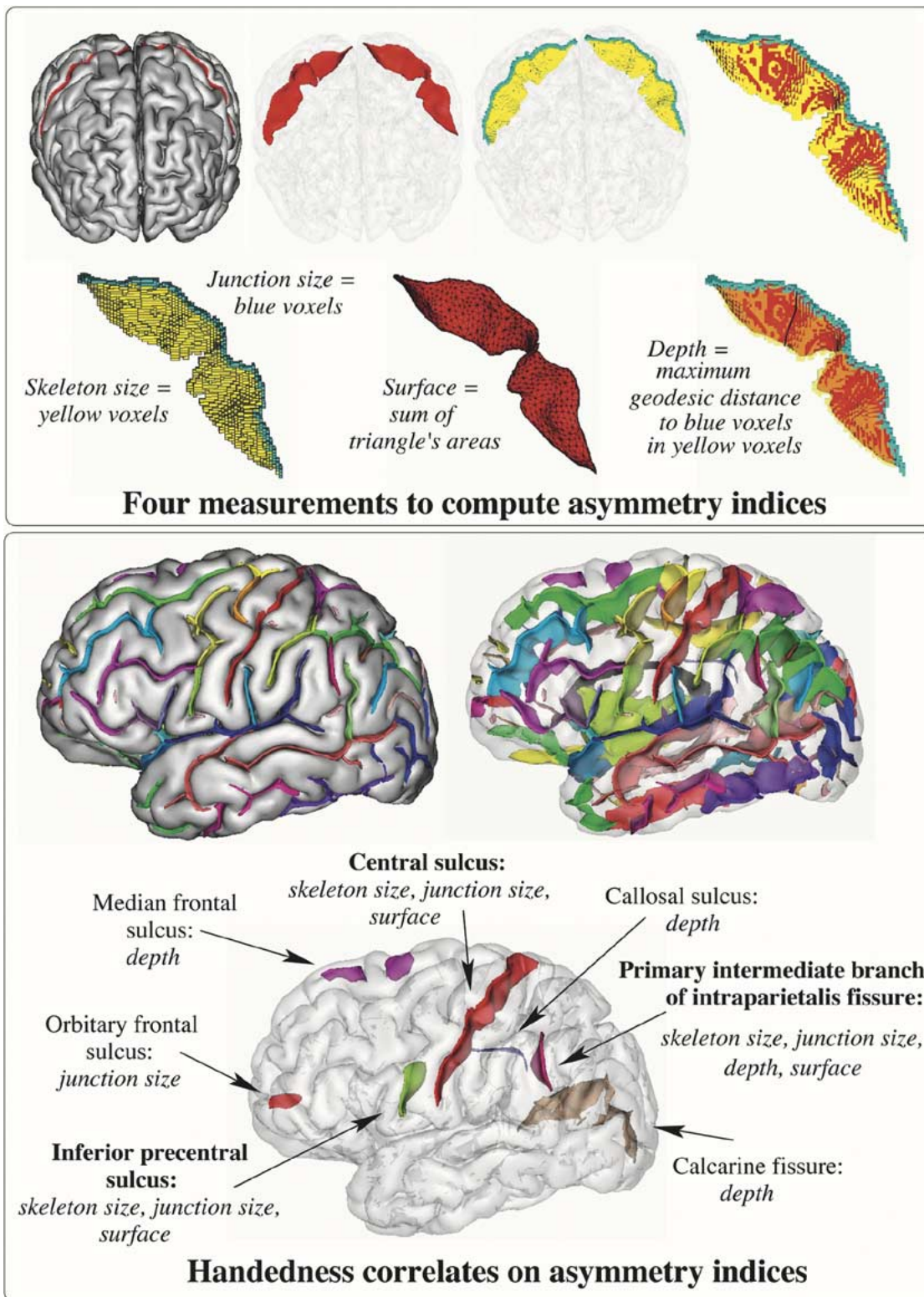


Fig. 4. (top) Each sulcus (here the central sulcus) is extracted in each hemisphere as a skeleton subset. In this figure, yellow voxels denote the main part of this subset, while cyan voxels correspond to the junction with the brain hull. This set of voxels is then meshed in order to have access to smooth 3-D rendering of the sulcus shape (red). Several morphometric measurements are inferred from the two types of representations. (bottom) 58 sulci have been identified in each brain. For each sulcus, an index of asymmetry is computed for each of the morphometric measurement. These indexes are compared across left-handed and right-handed populations. A few sulci lead to handedness correlated indexes. Their instances in one brain chosen randomly are highlighted in this figure, with the list of correlated indexes.

biased by the pose of this 3-D curve in Talairach's frame. It should be replaced in a near future by a better length estimation using geodesic distances.

- *The maximum geodesic depth of the sulcus.* This measurement is computed using a front-propagation based chamfer distance [80]. This depth corresponds to the

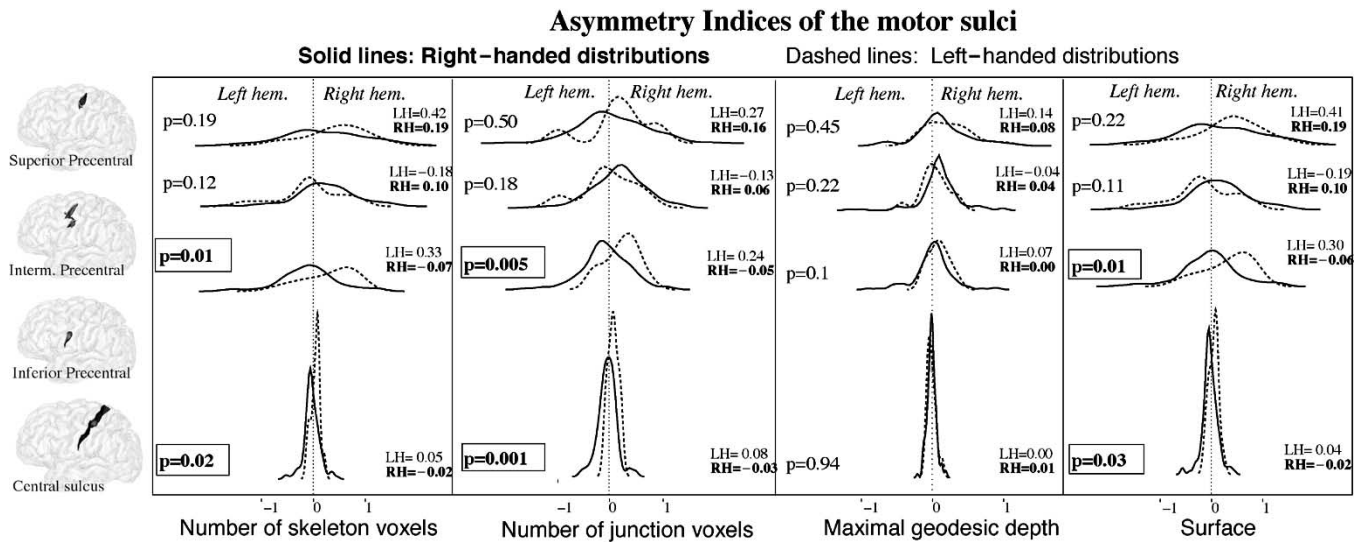


Fig. 5. The distributions of the four different asymmetry indexes are estimated for the four sulci delimiting the motor gyrus. A leftward asymmetry leads to negative indexes, while a rightward asymmetry leads to positive indexes. A T-test is used to compare left-handed and right-handed populations. The mean value of each index is also provided for each population (LH and RH). The framed p-values are considered as significant.

largest geodesic distance to the junction voxels computed inside the part of the skeleton representing the sulcus.

For each sulcus, a normalized asymmetry index  $((R - L)/(R + L)/2)$  was computed for each of these four measurements, where R (respectively, L) denotes the value in the right hemisphere (respectively, in the left hemisphere). For each sulcus, standard T-Tests were used to compare the asymmetry indexes of left-handed and right-handed groups, using a plug-in of brainVISA software (<http://brainvisa.info>) based on R software (<http://www.r-project.org/>). Several significant differences were revealed by our analysis ( $p < 0.05$ , see Fig. 4). For each result, we report the p-value and the mean asymmetry indexes for right-handed (RH) and left-handed (LH) groups:

*Primary intermediate branch of intraparietal fissure:*

- skeleton size:*  $p = 0.01$ , RH =  $-0.45$ , LH =  $0.11$ ;
- surface:*  $p = 0.01$ , RH =  $-0.49$ , LH =  $0.11$ ;
- junction size:*  $p = 0.003$ , RH =  $-0.33$ , LH =  $0.13$ ;
- depth:*  $p = 0.04$ , RH =  $-0.25$ , LH =  $0.00$ ;

*Central sulcus:*

- skeleton size:*  $p = 0.02$ , RH =  $-0.02$ , LH =  $0.05$ ;
- surface:*  $p = 0.03$ , RH =  $-0.02$ , LH =  $0.04$ ;
- junction size:*  $p = 0.001$ , RH =  $-0.03$ , LH =  $0.08$ ;

*Inferior precentral sulcus:*

- skeleton size:*  $p = 0.01$ , RH =  $-0.07$ , LH =  $0.33$ ;
- surface:*  $p = 0.01$ , RH =  $-0.06$ , LH =  $0.30$ ;
- junction size:*  $p = 0.005$ , RH =  $-0.05$ , LH =  $0.24$ ;

*Median frontal sulcus:*

- depth:*  $p = 0.01$ , RH =  $0.10$ , LH =  $-0.05$ ;

*Orbitary frontal sulcus:*

- junction size:*  $p = 0.03$ , RH =  $-0.31$ , LH =  $0.00$ ;

*Calcarine fissure:*

- depth:*  $p = 0.02$ , RH =  $0.02$ , LH =  $0.22$ ;

*Callosal sulcus:*

- depth:*  $p = 0.03$ , RH =  $0.05$ , LH =  $0.28$ ;

The three sulci leading to handedness correlates on several indexes present an asymmetry pattern left-right flipped between both groups: the sulcus is more developed in the hemisphere contralateral to the dominant hand. Two of these sulci (central

and inferior precentral) define the lowest part of the motor gyri. Since the motor areas are of course supposed to embed some handedness correlates, we focus the rest of our study on the four sulci defining the motor gyrus. For each of these sulci, the Fig. 5 provides the distributions of the asymmetry indexes for both populations. These distributions stem from the Gaussian kernel estimator of R software (<http://www.r-project.org/>). A T-test is used to compare both distributions.

It is interesting to note that the effects observed for the central sulcus are restricted to surface and length (size of the junction with the brain hull). The central sulcus depth, indeed, does not seem to be significantly influenced by handedness or hemisphere. This observation means that the increase in the central sulcus surface in the hemisphere contralateral to the dominant hand results only from an increase in the length of the sulcus. For the inferior precentral sulcus, depth is slightly asymmetric in the left-handed population, while no asymmetry is observed in the right-handed population. The superior and intermediate precentral sulci do not yield significant handedness correlates. The intermediate sulcus, however, presents a tendency to handedness correlates opposite to the pattern observed for the inferior precentral sulcus, namely a smaller sulcus in the hemisphere contralateral to the dominant hand. Finally, the superior sulcus has a tendency to be larger in the right hemisphere in both populations, this asymmetry being increased in the left-handed group.

The study described above addresses only handedness influence on asymmetry. The indexes used for this purpose have a good discriminative power because they are normalized relative to the size of the sulcus on an individual basis. Therefore, they discard the bias induced by the interindividual variability not removed by the affine normalization (the proportionalization) performed before sulcus extraction. In case of correlation of such an index with handedness, however, it is interesting to go back to the distributions of the normalized sizes of the sulcus in each hemisphere. Therefore, the Fig. 6 provides the distributions of surface and length for the four sulci delimiting the motor gyrus. Standard T-tests are performed to ask if these distributions differ between both populations. The results for the

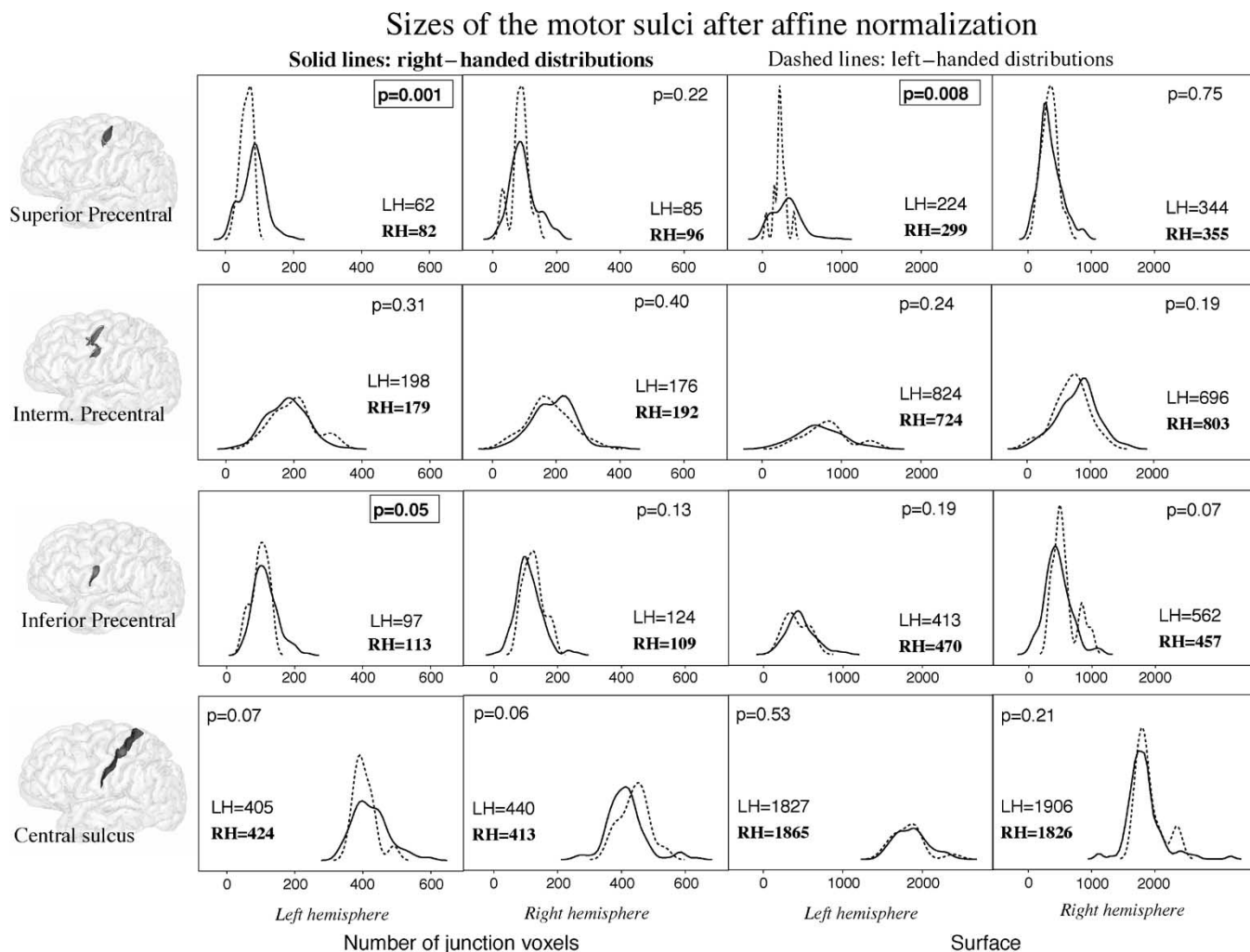


Fig. 6. The distributions of two different measurements are estimated for the four sulci delimiting the motor gyrus. For the two left columns, the unit is the number of junction voxels, while for the two right columns (sulcus surface) the unit is square millimeters. A T-test is used to compare left-handed and right-handed populations. The mean value of each index is also provided for each population (LH and RH). The framed p-values are considered as significant.

central sulcus show that handedness influence is stronger for the length of the sulcus than for the surface. The length distributions in each hemisphere, indeed, show close to significant handedness influence, while no effect is observed for the surface distribution. A surprising result occurs for the superior precentral sulcus, which is significantly larger in the left hemisphere in the right-handed population, while no handedness influence is observed in the right hemisphere. This observation shows clearly that some interesting information may be lost when using asymmetry indexes only. Finally, it should be noted that the affine normalization itself may not be the best way to perform the comparison of absolute sizes.

## V. DISCUSSION

It is too soon to discard the influence of various biases on the results mentioned above. For instance, the left-handed population is small but we have decided to stick to this dataset because it was used by a previous VBM study addressing the same question [81]. Some other bothering points are the small number of left-handed subjects (2) in the database used to train the pattern recognition system, or the possible differences between

both hemispheres introduced during the manual labeling of this database. Nevertheless, among the sulci presenting significant handedness correlates, two turn out to belong to the cortex area involved in motor control, which would have been the initial guess.

The central sulcus of right-handed subjects is larger in the left hemisphere which controls the right hand, while this pattern is flipped for left-handed subjects. A larger sulcus may simply result from the necessity to increase the local folding process in order to extend the size of the most active precentral motor gyrus. The same pattern is observed for the other boundary of the motor gyrus corresponding to the inferior precentral sulcus. Additionally, the left superior precentral sulcus is larger for right-handed subjects than for left-handed subjects. In return, the intermediate precentral sulcus which is folded orthogonally to the precentral gyrus, shows a tendency to be less developed in the most active hemisphere. A more detailed shape analysis has also shown that the left intermediate precentral sulcus of right handed subjects is more parallel to the central sulcus than in the case of left handed subjects, as if a larger development of the gyrus was pushing this orthogonal sulcus away [50]. This difference between inferior/superior precentral sulci

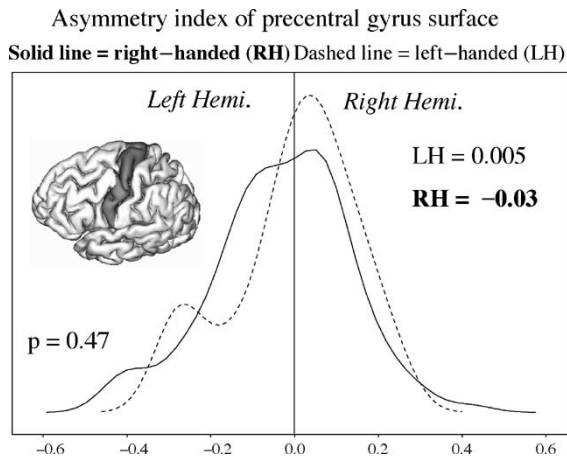


Fig. 7. The distributions of the asymmetry index computed for the precentral gyrus surface. A leftward asymmetry leads to negative indexes, while a rightward asymmetry leads to positive indexes. The mean value of each index is also provided for each population (LH and RH). A T-test used to compare left-handed and right-handed populations did not provide any significant result. However, the distributions show a tendency for larger motor gyrus surface in the dominant hemisphere.

versus intermediate precentral sulcus could also stem from their different embryological origin: the first ones are among the earliest folds to appear, while the intermediate sulcus results from a later “operculization,” namely the growth of one gyrus above a neighboring one.

Another interesting point lies in the two different ways of increasing the surface of a sulcus, through depth increase or length increase. In the case of the central sulcus, this second process appears dominating, which may provide some clues about the various constraints influencing the folding. These phenomena may be better understood from models of the various forces acting on the folding process when increasing the precentral gyrus surface [78]. Such studies, however, will require a further understanding of these forces, for instance through a better knowledge of the fiber bundles connecting the different motor areas obtained from diffusion imaging [49]. Interestingly, the handedness correlates are lower in the primary motor structures (central sulcus surface index:  $|RH - LH| = 6\%$ ) than in the structures responsible for planning and coordinating movements (inferior precentral sulcus surface index:  $|RH - LH| = 36\%$ ). Finally, it is also important to note that the pattern of asymmetry obtained for the central sulcus matches the results obtained by the majority of the manual studies [1], [2], [84].

In order to understand further the correlates of handedness on the sulcal patterns, we have applied to the whole database the method mentioned above for parcellation of the cortical surface into gyral patches. Twenty different gyri were defined from pairs of parallel sulci. Then, each gyrus surface was estimated from the sum of the triangles included into the corresponding Voronoi patch. The same kind of asymmetry indexes as the ones used for sulcus-based measurements were computed and compared across populations. None of these comparisons gave significant result. The distributions for precentral gyrus, however, show a tendency in accordance with the results obtained for the central and precentral sulci (see Fig. 7). Increasing the number of brains will be required to check whether this tendency can be confirmed. The amplitude of the effect, indeed,

may be hidden behind the variability of the gyrus segmentation induced by some weaknesses of our method. The definition of cortical gyri, anyway, is even more difficult than the definition of cortical sulci, which explains why we focused our first efforts on the second ones.

The only sulcus showing significant handedness correlates of its four asymmetry indexes is the primary intermediate branch of the intraparietalis fissure. This branch, which is sometimes also called the intermediate sulcus of Jensen, is a small highly variable fold embedded in the inferior parietal lobule, inside an area usually related to language in the left hemisphere (Wernicke’s area). This result can be easily related to one of the most intriguing results about handedness correlates: the fact that the planum temporale, a region of the posterior superior temporal lobe deeply involved in language understanding, shows marked leftward volume asymmetry which is greater for right-handed people [34], [68]. The planum temporale is defined relatively to the posterior part of the Sylvian fissure. Therefore, the planum is the anterior bank of a gyrus, whose posterior bank corresponds to the primary intermediate branch of the intraparietalis fissure. Hence, the asymmetry pattern observed for this branch, a large leftward asymmetry for right-handed subjects and a slight rightward asymmetry for left-handed subjects, is in harmony with the current knowledge.

The inverse asymmetries observed for the inferior and the intermediate precentral sulci raise one of the problems related to the object-based strategy: if the precentral sulcus had been defined as only one entity, the handedness correlate on its asymmetry may have been lost. In a similar way, our results do not highlight any direct handedness effect in the size of the planum temporale simply because the planum is not part of our cortex parcellation. These difficulties are related to the combinatorial outburst in the number of entities that could be defined to parcellate the cortex. In a way, this is the price to pay to have access to the better statistical power provided by the ROI-based strategy. This price is usually acceptable because the ROI definition is related to *a priori* knowledge of the scientist about his domain of interest. This is however questionable in the context of full parcellation of the cortex surface into sulci and gyri, considering the poor understanding of the link between these geometric structures and the underlying brain organization. At least, our system is based on a learning strategy which allows the user to define his own database of brains labeled according to his needs.

Another weakness of our strategy results from the purely geometric way of oversegmenting the cortex before gathering the different pieces, namely the elementary folds, into anatomical entities, namely the sulci. This prevents the definition of entities unrelated to these geometric features. This is one of the reasons why our framework can only be considered as a complementary window for cortical morphometry. The iconic normalization based strategy is more versatile since any template parcellation can be warped [18], [20]. This versatility results in fact from the lack of control on the localization of the template boundaries relatively to the individual anatomy after the warping process. This problem is very difficult to address when the template results from one single prototypical brain, without further knowledge about the interindividual variability of this parcellation. Representing this knowledge through probabilistic atlases of localization relative to the coordinate system has been one key direction of research during the last decade [55]. This

approach, however, loses important information like the statistical links between the parcellation boundaries and geometric features related to sulci. Therefore, it will be important to design more sophisticated statistical methods to represent this kind of relationships, which has been recently proposed by Fischl *et al.* in [28]. The challenge lies in the estimation of such statistics for the small database that can be usually afforded.

One issue which will require further study is whether a more sophisticated VBM approach than the one described in [81] may give access to the results obtained with the sulcus-based method. This VBM approach, indeed, involved only affine spatial normalization, which is far to be sufficient to align the central sulci. Therefore, a flipped 5% asymmetry in the sulcus size did not result in significant handedness correlates in the differences of tissue densities between both hemispheres, at least with only 14 left-handed brains. A non linear warping strategy could provide better results for the central sulcus, which is one of the less variable cortical structures. A recent comparative study, however, has shown the difficulties of sulcus alignment using only intensity-based similarity measures [35]. Anyway, a perfect alignment is not required to observe an effect but the observed effect may be sometimes misleading. As an illustration, Fig. 8 highlights handedness correlates on the localization of the central and precentral sulci in Talairach's frame after affine normalization. Such differences may lead to unpredictable results in VBM. In our opinion, the interpretation of VBM's statistical maps would be more reliable with additional statistical parametric maps of the sulcus localization after normalization.

The increase in statistical power provided by our ROI-based strategy leads to a loss of localization power. This is another reason why this approach should be associated with some coordinate-based approaches. The simplest idea consists in using the sulcus-based approach for mining the data, then perform more sophisticated local analysis. For instance, each sulcus can be endowed with a 2-D coordinate system in order to perform either local cortical thickness analysis or statistical shape modeling [24], [41], [70]. This structure-based local coordinate system strategy, unfortunately, does not deal nicely with the topological variability of the sulci. Therefore, it may be easier to apply the local coordinate systems to the gyri, which are usually non interrupted.

Considering the complexity of adapting a coordinate system to each cortical structure, an attractive alternative may consist in mixing warping and sulcus recognition in a hierarchical manner. A first affine registration may be used to constraint the recognition of the major sulci, following the strategy of our artificial neuroanatomist [62]. Then a non linear warping aligning these major sulci would result in a refined normalization [14], this new coordinate system being used to constraint the recognition of more variable sulci. This process could be iterated as long as new sulcal landmarks can be identified. It may also be used to guide the inference of new landmarks, either among the branches of the sulci or using another source of information like diffusion-weighted data. Diffusion imaging, indeed, may deeply modify the problem of intersubject alignment in a near future. This modality may provide new insight into the architectural subdivisions of the brain [40] which should be matched by iconic normalization. This has been shown for instance for the thalamus [6], [85]. It is bound to happen for the cortex, because fiber bundles will lead to architectural parcellations of the cor-

tical surface relatively to the connectivity patterns [69]. Finally, a new morphometry dedicated to the shapes of the bundles will have to be developed with an object-based strategy similar to the one described in this paper.

A last important weakness of our sulcus-based strategy is the lack of a brain-invariant generic model of the cortical folding patterns. Therefore, the manually labeled database which is the basis of our system embeds the subjectivity of our neuroanatomist. Hence, the automatic system is bound to reproduce this subjectivity, whatever the performance of the underlying pattern recognition system. Then, while the iconic normalization-based approach does not align perfectly the geometry of the cortex across subjects, our sulcus labeling is also far to be error prone. The two kinds of problems, however, stem from very different origins, which explains why they provide two complementary windows for the morphometry of the cortical shapes. An example of this complementarity has been shown recently through the study of the intraparietal sulcus in Turner syndrome [56]. It should be noted finally that while the current performance level of our system is not very impressive (25% of disagreement with the manual labeling), the results described in this paper have shown that this level is sufficient to perform meaningful observations.

Nevertheless, our main goal during the last 10 years has been the quest for a brain-invariant generic model, which would clarify the basis of cortical morphometry. While this may look like a hopeless Graal quest, this program of research has to be developed to reach at least partial answers [54]. We are convinced that the main source of understanding should stem from the study of the cortical folding process during brain growth. This process is now accessible through antenatal MR imaging, which may open the door to longitudinal studies if the ethical considerations are acceptable [10], [66]. Going back to the idea that a sulcus is a kind of character in the alphabet developed to describe the cortical folding patterns, we think that an enlightening analogy for the sulcus recognition is handwritten text recognition. With this point of view, sulci stand for words, that are sometimes difficult to split from one another. What we are looking for in the beginning of the cortical folding process is smaller indivisible entities called sulcal roots that may stand for the characters making up these words. These sulcal roots are the first folds appearing during brain growth [58]. They are supposed to be stable across subjects for genetic reasons. A sulcal root-based model would overcome the difficulties induced by sulcus interruptions. We are tracking the presence of these sulcal roots in the shape of adult brains through the study of the cortical surface curvature [11]. The gyri buried in the depth of the sulci, indeed, may correspond to the limits between these sulcal roots. We have developed a scale-space based method for the robust detection of these buried gyri, which will lead to refine the graph-based representations used by our system in a near future. The adaptation of the framework to sulcal root recognition is straightforward and has already been experimented with a poorer buried gyrus detection algorithm [61].

## VI. CONCLUSION

The object-based morphometry advocated in this paper will provide new insight into the forces sculpting the cortical folding

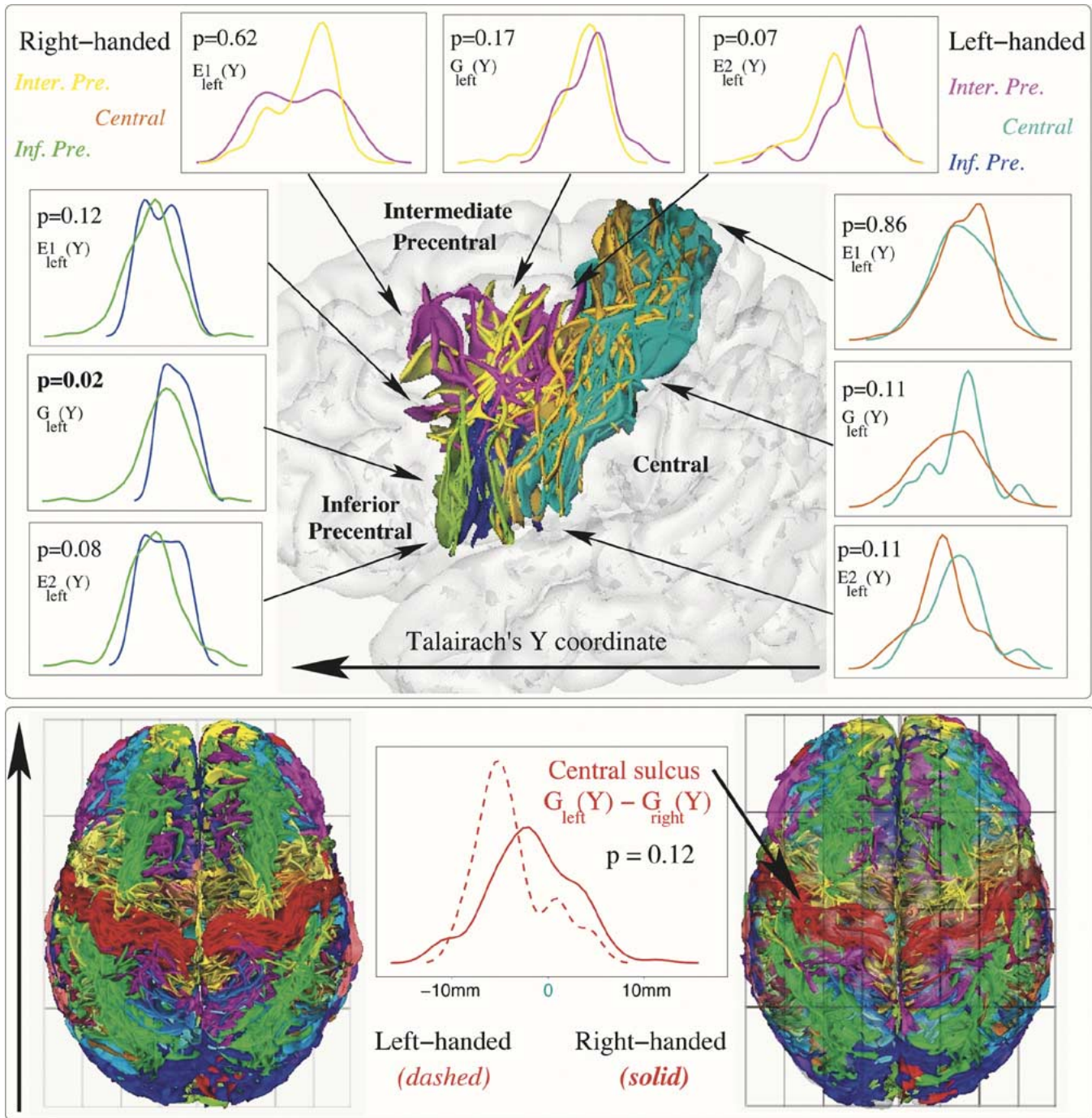


Fig. 8. (top) The central, inferior precentral and intermediate precentral sulci of left hemisphere for the 14 left-handed subjects and 14 right-handed subjects matched for sex and age. Each chart provides the distribution of the Y coordinate of one specific point in both populations. These points are either the sulcus center of mass or one of the two extremities of its junction with the brain hull. The p-values stem from standard t-tests comparing both populations. The lowest part of the left motor area of the left-handed population is located more posteriorly. (bottom) The sulci of the 14 left-handed subjects and 14 right-handed subjects randomly picked. The grid indicates Talairach's frame orientation. The chart plots the distributions of the discrepancy between the Y coordinates of the center of mass of left and right central sulci. A T-test is used to compare both populations. A backward displacement of the left central sulcus appears for both populations, with an increase in the left-handed population.

patterns. While the ROI-based strategy is often considered as a way to reduce morphometric information to a few numbers to be compared to the large amount of voxels underlying VBM, analysing the shapes of the sulcus-based ROIs leads to an opposite trend. Indeed, all the shape descriptors used by the sulcus recognition system can directly be used for morphometry. Shape descriptors dedicated to the surface parcellation can also be used, the simplest one being the gyral

patch areas. Considering that each of the 500 perceptrons involved in the sulcus recognition is fed by about 25 values, the sulcus patterns description includes about 12 500 numbers. Hence, some corrections will have to be developed to take into account the high risk of false positives implied by multiple testing, following the point of view developed for VBM using random field theory [86]. Such corrections, however, will be more difficult to perform because of the complex topology

of the underlying random fields. Fortunately, very different strategies can be developed to explore these data, which could partly overcome the problem. For instance, the feature selection methods classically developed to overcome the curse of dimensionality in classification may help to develop our sulcal pattern morphometry [25].

## REFERENCES

- [1] K. Amunts, L. Jäncke, H. Mohlberg, H. Steinmetz, and K. Zilles, "Interhemispheric asymmetry of the human motor cortex related to handedness and gender," *Neuropsychologia*, vol. 38, pp. 304–312, 2000.
- [2] K. Amunts, G. Schlaug, A. Schleicher, H. Steinmetz, A. Dabringhaus, P. E. Roland, and K. Zilles, "Asymmetry in the human motor cortex and handedness," *Neuroimage*, vol. 4, pp. 216–222, 1996.
- [3] J. Ashburner, J. G. Csernansky, C. Davatzikos, N. C. Fox, G. B. Frisoni, and P. M. Thompson, "Computer-assisted imaging to assess brain structure in healthy and diseased brains," *The Lancet Neurology*, vol. 2, 2003.
- [4] J. Ashburner and K. J. Friston, "Voxel-based morphometry—the methods," *NeuroImage*, vol. 11, pp. 805–821, 2000.
- [5] I. Biederman, "Recognition by components: a theory of human image understanding," *Psychological Rev.*, vol. 94, pp. 115–147, 1987.
- [6] T. E. Behrens, H. Johansen-Berg, M. W. Woolrich, S. M. Smith, C. A. Wheeler-Kingshott, P. A. Boulby, G. J. Barker, E. L. Sillery, K. Sheehan, O. Ciccarelli, A. J. Thompson, J. M. Brady, and P. M. Matthews, "Non-invasive mapping of connections between human thalamus and cortex using diffusion imaging," *Nat. Neurosci.*, vol. 6, no. 7, pp. 750–757, 2003.
- [7] W. Boling, A. Olivier, A. R. G. Bittar, and D. Reutens, "Localization of hand motor activation in Broca's pli de passage moyen," *J. Neurosurg.*, vol. 91, no. 6, pp. 903–910, 1999.
- [8] M. Brett, I. S. Johnsrude, and A. M. Owen, "The problem of functional localization in the human brain," *Nat. Rev. Neurosci.*, vol. 3, no. 3, pp. 243–249, 2002.
- [9] K. Brodmann, *Vergleichende Lokalisationslehre der Grosshirnrinde*. Leipzig, Germany: Barth, 1909.
- [10] A. Cachia, J.-F. Mangin, N. Boddaert, J. Régis, F. Kherif, P. Sonigo, M. Zilbovicius, I. Bloch, and F. Brunelle, "Study of cortical folding process with prenatal MR imaging," in *Proc. ISMRM*, Glasgow, Scotland, 2001, p. 121.
- [11] A. Cachia, J.-F. Mangin, D. Rivière, F. Kherif, N. Boddaert, A. Andrade, D. Papadopoulos-Orfanos, J.-B. Poline, I. Bloch, M. Zilbovicius, P. Sonigo, F. Brunelle, and J. Régis, "A primal sketch of the cortex mean curvature: a morphogenesis based approach to study the variability of the folding patterns," *IEEE Trans. Med. Imag.*, vol. 22, pp. 754–765, June 2003.
- [12] A. Cachia, J.-F. Mangin, D. Rivière, D. Papadopoulos-Orfanos, F. Kherif, I. Bloch, and J. Régis, "A generic framework for parcellation of the cortical surface into gyri using geodesic Voronoi diagrams," *Med. Image Anal.*, vol. 7, no. 4, pp. 403–416, 2003.
- [13] P. Cachier, E. Bardinet, D. Dormont, X. Pennec, and N. Ayache, "Iconic feature based nonrigid registration: the PASHA algorithm," *Proc. CVIU*, vol. 89, no. 2–3, pp. 272–298, 2003.
- [14] P. Cachier, J.-F. Mangin, X. Pennec, D. Rivière, D. Papadopoulos-Orfanos, J. Régis, and N. Ayache, "Multisubject nonrigid registration of brain MRI using intensity and geometric features," in *Lecture Notes in Computer Science*. Utrecht, The Netherlands: Springer-Verlag, 2001, vol. 2208, MICCAI, pp. 734–742.
- [15] A. Caunce and C. J. Taylor, "Building 3D sulcal models using local geometry," *Med. Image Anal.*, vol. 5, no. 1, pp. 69–80, 2001.
- [16] H. Chui, L. Win, R. Schultz, J. S. Duncan, and A. Rangarajan, "A unified nonrigid feature registration method for brain mapping," *Med. Image Anal.*, vol. 7, no. 2, pp. 113–130, 2003.
- [17] M. K. Chung, K. J. Worsley, T. Paus, C. Cherif, D. L. Collins, J. N. Giedd, J. L. Rapoport, and A. C. Evans, "A unified statistical approach to deformation-based morphometry," *NeuroImage*, vol. 14, no. 3, pp. 595–606, 2001.
- [18] D. L. Collins and A. C. Evans, "Animal: validation and applications of nonlinear registration-based segmentation," *Proc. IJPRAI*, vol. 11, no. 8, pp. 1271–1294, 1997.
- [19] D. L. Collins, G. Le Goualher, and A. C. Evans, "Non-linear cerebral registration with sulcal constraints," in *Lecture Notes in Computer Science*, vol. 1496, MICCAI'98. Berlin, Germany, 1998, pp. 974–984.
- [20] D. L. Collins, C. J. Holmes, T. M. Peters, and A. C. Evans, "Automatic 3D model-based neuroanatomical segmentation," *Hum. Brain Mapp.*, vol. 3, no. 3, pp. 190–208, 1995.
- [21] D. L. Collins, P. Neelin, T. M. Peters, and A. C. Evans, "Automatic 3D intersubject registration of MR volumetric data in standardized Talairach space," *J. Comput. Assist. Tomogr.*, vol. 18, no. 2, pp. 192–205, 1994.
- [22] F. Crivello, T. Schormann, N. Tzourio-Mazoyer, P. E. Roland, K. Zilles, and B. M. Mazoyer, "Comparison of spatial normalization procedures and their impact on functional maps," *Hum. Brain Mapp.*, vol. 16, no. 4, pp. 228–250, 2002.
- [23] C. Davatzikos and R. N. Bryan, "Morphometric analysis of cortical sulci using parametric ribbons: a study of the central sulcus," *J. Comput. Assist. Tomogr.*, vol. 26, no. 2, pp. 298–307, 2002.
- [24] R. H. Davies, C. Twining, T. F. Cootes, and C. J. Taylor, "A minimum description length approach to statistical shape modeling," *IEEE Trans. Med. Imag.*, vol. 21, pp. 525–537, May 2002.
- [25] E. Duchesnay, A. Roche, D. Rivière, D. Papadopoulos-Orfanos, Y. Coindes, and J.-F. Mangin, "Population classification based on structural morphometry of cortical sulci," in *Proc. 2th ISBI*, Arlington, VA, 2004, pp. 1276–1279.
- [26] B. Fischl and A. M. Dale, "Measuring the thickness of the human cerebral cortex from magnetic resonance images," *Proc. Nat. Acad. Sci. USA*, vol. 97, no. 20, pp. 11 050–11 055, 2000.
- [27] B. Fischl, M. I. Sereno, R. B. Tootle, and A. M. Dale, "High-resolution intersubject averaging and a coordinate system for the cortical surface," *Hum. Brain Mapp.*, vol. 8, no. 4, pp. 272–284, 1999.
- [28] B. Fischl, A. Van Der Kouwe, C. Destrieux, E. Halgren, F. Segonne, D. H. Salat, E. Busa, L. J. Seidman, J. Goldstein, D. Kennedy, V. Caviness, N. Makris, B. Rosen, and A. M. Dale, "Automatically parcellating the human cerebral cortex," *Cereb. Cortex*, vol. 14, no. 1, pp. 11–22, 2004.
- [29] P. Fox, J. Perlmutter, and M. Raichle, "A stereotactic method of anatomical localization for PET," *J. Comput. Assist. Tomogr.*, vol. 9, pp. 141–153, 1985.
- [30] K. Friston, J. Ashburner, J.-B. Poline, C. D. Frith, J. D. Heather, and R. S. J. Frackowiak, "Spatial realignment and normalization of images," *Hum. Brain Mapp.*, vol. 2, pp. 165–189, 1995.
- [31] S. Geman and D. Geman, "Stochastic relaxation, Gibbs distributions and the bayesian restoration of images," *IEEE Trans. Pattern Anal. Machine Intell.*, vol. 6, pp. 721–741, Nov. 1984.
- [32] C. D. Good, I. Johnsrude, J. Ashburner, R. N. A. Henson, K. J. Friston, and R. S. J. Frackowiak, "Cerebral asymmetry and the effects of sex and handedness on brain structure: a voxel-based morphometric analysis of 465 normal adult human brains," *Neuroimage*, vol. 14, pp. 685–700, 2001.
- [33] A. Guimond, A. Roche, N. Ayache, and J. Meunier, "Multimodal brain warping using the demons algorithm and adaptive intensity corrections," *IEEE Trans. Med. Imag.*, vol. 20, pp. 58–69, Jan. 2001.
- [34] M. Habib, F. Robichon, O. Levrier, R. Khalil, and G. Salamon, "Diverging asymmetries of temporo-parietal cortical areas: a reappraisal of Geschwind/Galaburda theory," *Brain Lang.*, vol. 48, no. 2, pp. 238–258, 1995.
- [35] P. Hellier and C. Barillot, "Coupling dense and landmark-based approaches for nonrigid registration," *IEEE Trans. Med. Imag.*, vol. 22, pp. 217–227, Feb. 2003.
- [36] P. Hellier, C. Barillot, I. Corouge, B. Gibaud, G. Le Goualher, D. L. Collins, A. C. Evans, G. Malandain, N. Ayache, G. E. Christensen, and H. J. Johnson, "Retrospective evaluation of intersubject brain registration," *IEEE Trans. Med. Imag.*, vol. 22, pp. 1120–1130, Sept. 2003.
- [37] P. Hellier, C. Barillot, E. Memin, and P. Perez, "Hierarchical estimation of a dense deformation field for 3-d robust registration," *IEEE Trans. Med. Imag.*, vol. 20, pp. 388–402, May 2001.
- [38] H. J. Johnson and G. E. Christensen, "Consistent landmark and intensity-based image registration," *IEEE Trans. Med. Imag.*, vol. 21, pp. 450–461, May 2002.
- [39] P. Kochunov, J. Lancaster, P. Thompson, A. W. Toga, P. Brewer, J. Hardies, and P. Fox, "An optimized individual target brain in the Talairach coordinate system," *Neuroimage*, vol. 17, no. 2, pp. 922–927, 2002.
- [40] D. Le Bihan, J.-F. Mangin, C. Poupon, C. A. Clark, S. Pappata, N. Molko, and H. Chabriat, "Diffusion tensor imaging: concepts and applications," *J. Magn. Reson. Imag.*, vol. 13, pp. 534–546, 2001.
- [41] G. Le Goualher, A. M. Argenti, M. Duyme, W. F. Baare, H. E. Hulshoffpool, D. I. Boomsma, A. Zouaoui, C. Barillot, and A. C. Evans, "Statistical sulcal shape comparisons: application to the detection of genetic encoding of the central sulcus shape," *Neuroimage*, vol. 11, no. 5, pp. 564–574, 2000.
- [42] G. Le Goualher, C. Barillot, and Y. Bizais, "Modeling cortical sulci using active ribbons," *Int. J. Pattern Recognit. Artif. Intell.*, vol. 11, no. 8, pp. 1295–1315, 1997.
- [43] G. Le Goualher, E. Procyk, D. L. Collins, R. Venugopal, C. Barillot, and A. C. Evans, "Automated extraction and variability analysis of sulcal neuroanatomy," *IEEE Trans. Med. Imag.*, vol. 18, pp. 206–217, Mar. 1999.

- [44] G. Lohmann and D. Y. von Cramon, "Automatic labeling of the human cortical surface using sulcal basins," *Med. Image Anal.*, vol. 4, no. 3, pp. 179–188, 2000.
- [45] D. Mac Donald, N. Kabani, D. Avis, and A. C. Evans, "Automated 3-D extraction of inner and outer surfaces of cerebral cortex from MRI," *Neuroimage*, vol. 12, no. 3, pp. 340–356, 2000.
- [46] J.-F. Mangin, "Entropy minimization for automatic correction of intensity nonuniformity," in *Proc. IEEE Workshop MMBIA*, Hilton Head Island, S.C., 2000, pp. 162–169.
- [47] J.-F. Mangin, O. Coulon, and V. Frouin, "Robust brain segmentation using histogram scale-space analysis and mathematical morphology," in *Lecture Notes in Computer Science*, W. M. Wells, A. Colchester, and S. Delp, Eds. Boston, MA: Springer-Verlag, Oct. 1998, vol. 1496, Proc. 1st MICCAI, pp. 1230–1241.
- [48] J.-F. Mangin, V. Frouin, I. Bloch, J. Régis, and J. López-Krahe, "3D magnetic resonance images to structural representations of the cortex topography using topology preserving deformations," *J. Math. Imag. Vis.*, vol. 5, no. 4, pp. 297–318, 1995.
- [49] J.-F. Mangin, C. Poupon, Y. Cointepas, D. Rivière, D. Papadopoulos-Orfanos, C. A. Clark, J. Régis, and D. Le Bihan, "A framework based on spin glass models for the inference of anatomical connectivity from diffusion-weighted MR data," *NMR Biomed.*, vol. 15, pp. 481–492, 2002.
- [50] J.-F. Mangin, F. Poupon, D. Rivière, D. L. Collins, A. C. Evans, and J. Régis, "3D moment invariant based morphometry," in *Lecture Notes in Computer Science*. Berlin, Germany: Springer-Verlag, 2003, vol. 2879, Proc. MICCAI, pp. 505–512.
- [51] J.-F. Mangin, J. Régis, I. Bloch, V. Frouin, Y. Samson, and J. Lopez-Krahe, "A Markovian random field based random graph modeling the human cortical topography," in *Lecture Notes in Computer Science*, vol. 905, CVRMed. Berlin, Germany, 1995, pp. 177–183.
- [52] J.-F. Mangin, J. Régis, and V. Frouin, "Shape bottlenecks and conservative flow systems," in *Proc. IEEE Workshop MMBIA*, San Francisco, CA, 1996, pp. 319–328.
- [53] J.-F. Mangin, D. Rivière, A. Cachia, D. Papadopoulos-Orfanos, D. L. Collins, A. C. Evans, and J. Régis, "Object-based strategy for morphometry of the cerebral cortex," in *Lecture Notes in Computer Science*. Berlin, Germany: Springer Verlag, 2003, vol. 2732, Proc. IPMI, pp. 160–171.
- [54] J.-F. Mangin, D. Rivière, O. Coulon, C. Poupon, A. Cachia, Y. Cointepas, J.-B. Poline, D. Le Bihan, J. Régis, and D. Papadopoulos-Orfanos, "Coordinate-based versus structural approaches to brain image analysis," *Artif. Intell. Med.*, vol. 30, pp. 177–197, 2004.
- [55] J. Mazziotta, A. Toga, A. Evans, P. Fox, J. Lancaster, K. Zilles, R. Woods, T. Paus, G. Simpson, B. Pike, C. Holmes, L. Collins, P. Thompson, D. MacDonald, M. Iacoboni, T. Schormann, K. Amunts, N. Palomero-Gallagher, S. Geyer, L. Parsons, K. Narr, N. Kabani, G. Le Goualher, D. Boomsma, T. Cannon, R. Kawashima, and B. Mazoyer, "A probabilistic atlas and reference system for the human brain: International consortium for brain mapping (ICBM)," *Philos. Trans. Roy. Soc. Lond. B Biol. Sci.*, vol. 356, no. 1412, pp. 1293–1322, 2001.
- [56] N. Molko, A. Cachia, D. Rivière, J.-F. Mangin, M. Bruandet, D. Le Bihan, L. Cohen, and S. Dehaene, "Functional and structural alterations of the intraparietal sulcus in a developmental dyscalculia of genetic origin," *Neuron*, vol. 40, pp. 847–858, 2003.
- [57] M. Ono, S. Kubik, and C. D. Abernathy, *Atlas of the Cerebral Sulci*. Stuttgart, Germany: Thieme Verlag, 1990.
- [58] J. Régis, J.-F. Mangin, V. Frouin, F. Sastre, J. C. Peragut, and Y. Samson, "Generic model for the localization of the cerebral cortex and preoperative multimodal integration in epilepsy surgery," *Stereotactic Functional Neurosurg.*, vol. 65, pp. 72–80, 1995.
- [59] M. E. Rettmann, X. Han, C. Xu, and J. L. Prince, "Automated sulcal segmentation using watersheds on the cortical surface," *NeuroImage*, vol. 15, no. 2, pp. 329–344, 2002.
- [60] M. Riesenhuber and T. Poggio, "Neural mechanisms of object recognition," *Curr. Opin. Neurobiol.*, vol. 12, pp. 162–168, 2002.
- [61] D. Rivière, "Apprentissage de la variabilité inter-individuelle de l'anatomie corticale cérébrale pour la reconnaissance automatique des sillons," Ph.D. thesis, Univ. d'Évry Val d'Essonne, Évry, France, 2000.
- [62] D. Rivière, J.-F. Mangin, D. Papadopoulos-Orfanos, J.-M. Martinez, V. Frouin, and J. Régis, "Automatic recognition of cortical sulci of the human brain using a congregation of neural networks," *Med. Image Anal.*, vol. 6, no. 2, pp. 77–92, 2002.
- [63] N. Royackkers, M. Desvignes, H. Fawal, and M. Revenu, "Detection and statistical analysis of human cortical sulci," *NeuroImage*, vol. 10, pp. 625–641, 1999.
- [64] D. Rueckert, A. F. Frangi, and J. A. Schnabel, "Automatic construction of 3-d statistical deformation models of the brain using nonrigid registration," *IEEE Trans. Med. Imag.*, vol. 22, pp. 1014–1025, Aug. 2003.
- [65] T. Schormann and M. Kraemer, "Voxel-guided morphometry ("vgm") and application to stroke," *IEEE Trans. Med. Imag.*, vol. 22, pp. 62–74, Jan. 2003.
- [66] P. Scifo, A. Cachia, N. Boddaert, P. Sonigo, I. Simon, M. Zilbovicius, F. Lethimonnier, D. Le Bihan, F. Brunelle, and J.-F. Mangin, "Antenatal MR imaging for the study of fetus brain development," in *Proc. 9th HBM, Neuroimage*, vol. 19, 2003, p. 1589.
- [67] D. Shen and C. Davatzikos, "Hammer: hierarchical attribute matching mechanism for elastic registration," *IEEE Trans. Med. Imag.*, vol. 21, pp. 1421–1439, Nov. 2002.
- [68] H. Steinmetz, "Structure, functional and cerebral asymmetry: in vivo morphometry of the planum temporale," *Neurosci. Biobehav. Rev.*, vol. 20, no. 4, pp. 587–591, 1996.
- [69] K. E. Stephan, K. Zilles, and R. Kötter, "Coordinate-independent mapping of structural and functional data by objective relational transformation (ORT)," *Phil. Trans. Roy. Soc. Lond. B*, vol. 355, pp. 37–54, 2000.
- [70] M. Styner, G. Gerig, J. Lieberman, D. Jones, and D. Weinberger, "Statistical shape analysis of neuroanatomical structures based on medial models," *Med. Image Anal.*, vol. 7, no. 3, pp. 207–220, 2003.
- [71] J. Talairach, G. Szikla, P. Tournoux, A. Prosalentis, and M. Bordas-Ferrier, *Atlas d'Anatomie Stéréotaxique du Téleencéphale*. Paris, France: Masson, 1967.
- [72] P. Thompson and A. W. Toga, "A surface-based technique for warping three-dimensional images of the brain," *IEEE Med. Imag.*, vol. 15, pp. 402–417, Aug. 1996.
- [73] P. M. Thompson, R. P. Woods, M. S. Mega, and A. W. Toga, "Mathematical/computational challenges in creating deformable and probabilistic atlases of the human brain," *Hum. Brain Mapp.*, vol. 9, no. 2, pp. 81–92, 2000.
- [74] A. W. Toga and P. M. Thompson, "New approaches in brain morphometry," *Amer. J. Geriatr. Psych.*, vol. 10, no. 1, pp. 13–23, 2002.
- [75] —, "Mapping brain asymmetry," *Nature Neurosci. Rev.*, vol. 4, no. 1, pp. 37–48, 2003.
- [76] S. Ullman, M. Vidal-Naquet, and E. Sali, "Visual features of intermediate complexity and their use in classification," *Nature Neurosci.*, vol. 5, no. 7, pp. 682–687, 2002.
- [77] M. Vaillant and C. Davatzikos, "Finding parametric representations of the cortical sulci using active contour model," *Med. Image Anal.*, vol. 1, no. 4, pp. 295–315, 1997.
- [78] D. C. Van Essen, "A tension-based theory of morphogenesis and compact wiring in the central nervous system," *Nature*, vol. 385, pp. 313–318, 1997.
- [79] D. C. Van Essen, H. A. Drury, S. Joshi, and M. I. Miller, "Functional and structural mapping of human cerebral cortex: solutions are in the surfaces," *Proc. Nat. Acad. Sci. USA*, vol. 95, no. 3, pp. 788–795, 1998.
- [80] B. J. H. Verwer, P. W. Verbeek, and S. T. Dekker, "An efficient uniform cost algorithm applied to distance transforms," *IEEE Trans. Pattern Anal. Machine Intell.*, vol. 11, pp. 425–428, Apr. 1989.
- [81] K. E. Watkins, T. Paus, J. P. Lerch, A. Zijdenbos, D. L. Collins, P. Neelin, J. Taylor, K. J. Worsley, and A. C. Evans, "Structural asymmetries in the human brain: a voxel-based statistical analysis of 142 mri scans," *Cereb. Cortex*, vol. 11, no. 9, pp. 868–877, 2001.
- [82] W. Welker, "Why does cerebral cortex fissure and fold?," in *Cerebral Cortex*. New York: Plenum, 1988, vol. 8B, pp. 3–135.
- [83] L. E. White, T. J. Andrews, C. Hulette, A. Richards, M. Groelle, J. Paydafar, and D. Purves, "Structure of the human sensorimotor system. ii: lateral symmetry," *Cereb. Cortex*, vol. 7, pp. 31–47, 1997.
- [84] L. E. White, G. Lucas, A. Richards, and D. Purves, "Cerebral asymmetry and handedness," *Nature*, vol. 368, pp. 197–198, 1994.
- [85] M. R. Wiegell, D. S. Tuch, H. B. W. Larsson, and V. J. Wedeen, "Automatic segmentation of thalamic nuclei from diffusion tensor magnetic resonance imaging," *Neuroimage*, vol. 19, no. 2, pp. 391–401, 2003.
- [86] K. Worsley, "The geometry of random images," *Chance*, vol. 9, no. 1, pp. 27–40, 1996.
- [87] T. A. Yousry, U. D. Schmid, H. Alkadhi, D. Schmidt, A. Peraud, A. Buettner, and P. Winkler, "Localization of the motor hand area to a knob on the precentral gyrus. A new landmark," *Brain*, vol. 120, no. 1, pp. 141–157, 1997.
- [88] X. Zeng, L. H. Staib, R. T. Schultz, H. Tagare, L. Win, and J. S. Duncan, "A new approach to 3D sulcal ribbon finding from MR images," in *Lecture Notes in Computer Science*. Berlin, Germany: Springer-Verlag, 1999, vol. 1679, Proc. MICCAI'99, pp. 148–157.